Lipidomics reveals that adiposomes store ether lipids and mediate phospholipid traffic[1],[s]

René Bartz,* Wen-Hong Li,* Barney Venables,[†] John K. Zehmer,* Mary R. Roth,[§] Ruth Welti,[§] Richard G. W. Anderson,* Pingsheng Liu,[1,2,*] and Kent D. Chapman[2,†]

Department of Cell Biology,* University of Texas Southwestern Medical Center, Dallas, TX 75390-9039; Center for Plant Lipid Research,[†] Department of Biological Sciences, University of North Texas, Denton, TX 76203-1277; and Kansas Lipidomics Research Center,[§] Division of Biology, Kansas State University, Manhattan, KS 66506

Abstract **Lipid droplets are accumulations of neutral lipids surrounded by a monolayer of phospholipids and associated proteins. Recent proteomic analysis of isolated droplets suggests that they are part of a dynamic organelle system that is involved in membrane traffic as well as packaging and distributing lipids in the cell. To gain a better insight into the function of droplets, we used a combination of mass spectrometry and NMR spectroscopy to characterize the lipid composition of this compartment. In addition to cholesteryl esters and triacylglycerols with mixed fatty acid composition, we found that ~10–20% of the neutral lipids were the ether lipid monoalk(en)yl diacylglycerol. Although lipid droplets contain only 1–2% phospholipids by weight, >160 molecular species were identified and quantified. Phosphatidylcholine (PC) was the most abundant class, followed by phosphatidylethanolamine (PE), phosphatidylinositol, and ether-linked phosphatidylcholine (ePC). Relative to total membrane, droplet phospholipids were enriched in lysoPE, lysoPC, and PC but deficient in sphingomyelin, phosphatidylserine, and phosphatidic acid.** These results suggest that droplets play a central role in ether lipid metabolism and intracellular lipid traffic.—Bartz, R., W-H. Li, B. Venables, J. K. Zehmer, M. R. Roth, R. Welti, R. G. W. Anderson, P. Liu, and K. D. Chapman. **Lipidomics reveals that adiposomes store ether lipids and mediate phospholipid traffic.** *J. Lipid Res.* 2007. **48:** 837–847.

Supplementary key words lipid droplet • membranes • phospholipid turnover

Lipid droplets are recognized by their conserved structural organization, which consists of a hydrophobic matrix of neutral lipid covered by a monolayer of phospholipids and associated proteins (1). Although traditionally regarded as a simple repository for stored carbon reserves, emerging evidence suggests that droplets function as dynamic organelles with a central role in cellular lipid metabolism, membrane trafficking, and cell signaling (2). Because lipid droplets can be found in bacteria, yeast, plant, and animal cells, over the years they have acquired a variety of names. Recently, we proposed that this diverse collection of names be replaced with the designation adiposome (3). Thus, an adiposome is an organelle that is specialized for packaging and distributing lipids in cells. In this nomenclature, the droplet is simply the most visible stage in the complex life cycle of an adiposome.

During the past few years, a number of reports have focused on the protein composition of lipid droplets isolated from yeast (4), plant (5), and animal (3, 6, 7) cells. A consensus view from these studies is that droplets contain structural proteins, proteins involved in the biosynthesis and breakdown of lipids, and proteins that mediate membrane traffic. Thus, the proteome indicates that droplets are actively engaged in membrane traffic, perhaps for the purpose of maintaining the proper lipid composition of different membrane compartments. In contrast to the proteins, surprisingly little is known about the lipid composition of animal cell droplets. Generally, droplets are rich in neutral lipids such as triacylglycerol (TAG) and cholesteryl esters that have a diverse population of esterified fatty acids (8). Here, we report an analysis of the lipid composition of droplets purified from various types of cultured and tissue cells. We used a combination of NMR spectroscopy and mass spectrometric approaches [including high-throughput, direct infusion electrospray ionization-tandem mass spectrometry (ESI-MS/MS)] to characterize the neutral lipid and phospholipid composition of isolated droplets. We found that droplets are rich not only in TAG and cholesteryl esters esterified with a variety of different fatty acids but also in the ether neutral lipid monoalk(en)yl diacylglycerol

[1] These two groups contributed equally to the project (Group 1: Bartz, Li, Zehmer, Anderson, and Liu; Group 2: Venables, Roth, Welti, and Chapman).

[2] To whom correspondence should be addressed.
e-mail: chapman@unt.edu (K.D.C.); pingsheng.liu@southwestern.edu (P.L.)
[s] The online version of this article (available at http://www.jlr.org) contains supplemental data in the form of 3 tables and 4 figures.

(MADAG). Despite representing only 1–2% of the total lipid in the droplet, the phospholipid composition included diverse molecular species of phosphatidylcholine (PC), phosphatidylethanolamine (PE), phosphatidylinositol (PI), ether-linked phosphatidylcholine (ePC), and ether-linked phosphatidylethanolamine (ePE) but very little phosphatidylserine (PS) or sphingomyelin (SM). We identified and quantified >160 phospholipid molecular species, which suggests that the simple phospholipid monolayer surrounding each droplet has an amazingly complex lipid composition. The neutral and phospholipid composition of lipid droplets is consistent with adiposomes having a direct role in lipid metabolism and in the intracellular traffic of membrane lipids.

MATERIALS AND METHODS

Materials

FBS and cosmic calf serum were from Hyclone (Logan, UT). DMEM and oleate were from Sigma (St. Louis, MO). Silica gel TLC plates were from Whatman (Brentford, Middlesex, UK).

Tissue culture

CHO K2 cells were cultured on 150 mm plates with 25 ml of DMEM (high-glucose; 4.5 g/l) containing 10% cosmic calf serum, 40 μg/ml proline, 100 U/ml penicillin, and 100 μg/ml streptomycin. Immortalized human B lymphocytes were cultured in RPMI 1640 containing 10% FBS as described previously (9). 3T3-L1 cells, primary human fibroblasts, fibroblasts derived from Zellweger patients (No. GM04340; Coriell Cell Repositories, Camden, NJ), NRK cells, and immortalized human fibroblasts (SV589 cells) were maintained in DMEM (low-glucose; 2.5 g/l) and 10% FBS supplemented with 100 U/ml penicillin and 100 μg/ml streptomycin. Lipid droplets were induced by incubating confluent cells in the presence of 100 μM oleate for NRK cells or 80 μM oleate for other cells for either 48 h for primary human fibroblasts or 16 h for other cells. 3T3-L1 cells were induced to differentiate by incubating them in the presence of 10 μg/ml insulin, 1 μM dexamethasone, and 200 μM isobutylxanthine (Sigma) for 48 h followed by insulin alone for an additional 4 days with a medium change after 2 days.

Lipid extraction and TLC

For mass spectrometry and NMR analysis, lipids were extracted into $CHCl_3$ from droplet fractions or whole cells by a modification of the Bligh and Dyer method (10) in which methanol was replaced with 2-propanol (11). Monophasic extracts were partitioned into two phases, and the organic layer was washed three times with 1 M KCl (12). Total lipid mass was estimated gravimetrically after removing solvent under a gentle stream of N_2 gas. Lipids were extracted from lipid droplets of tissue cultured cells and mouse liver or from 20 mg of adipose tissue for TLC analysis of unknown neutral lipid using $CHCl_3$/acetone (1:1, v/v). The solvent was removed by N_2 gas, and the lipids were dissolved in $CHCl_3$ and separated on TLC plates in hexane-diethyl ether-acetic acid (80:20:1, v/v) for 40 min. Lipid classes were visualized by iodine vapor or charring and semiquantified by densitometric scanning (NIH ImageJ software). Neutral lipid classes were quantified (and identified) according to TLC standards (Nu-Chek Prep, Inc., Elysian, MN) and separated under the same conditions at different amounts to generate standard curves for each major lipid class. In some cases, total lipid extracts were dissolved in $CHCl_3$ for LC-MS analysis or phospholipid profiling. In some cases, TLC was used to separate neutral lipid classes that were then recovered from silica gel in acidified $CHCl_3$ without exposure of lipids to iodine vapor.

Liquid chromatography and atmospheric pressure chemical ionization mass spectrometry

A nonpolar lipid fraction migrating between TAGs and cholesteryl esters was isolated by TLC and recovered in $CHCl_3$ as described above. Fractions were examined for ionization by direct infusion using ESI and atmospheric pressure chemical ionization (APCI) in both positive and negative ion modes. The strongest ionization was observed with positive ion APCI, which was then coupled with reverse-phase liquid chromatography. An Agilent (Palo Alto, CA) 1100 LC-MS system with a model SL ion trap mass spectrometer was operated with a Zorbax C18 column (2.1 × 150 mm; 5 μm particle size) and isocractic mobile phase of 1:1 methanol-dichloromethane at 0.3 ml/min. Peaks with major ions corresponding to those seen by direct infusion eluted in <10 min. MS conditions were as follows: nebulizer pressure = 60 p.s.i., dry gas flow = 5 l/min, dry gas temperature = 350°C, vaporization temperature = 425°C, corona current = 4,000 nA, and capillary voltage = 3,500 V.

Ether-neutral lipid identification by matrix-assisted laser desorption-time of flight mass spectrometry

Neutral lipid classes from ∼100 mg of adiposome lipids were fractionated by low-pressure flash chromatography on silica gel G60 (63 to ∼200 μm; EM Science, Gibbstown, NJ) and eluted with hexane-diethyl ether (30:1, v/v). Three major fractions corresponding to cholesteryl esters, ether-neutral lipids, and TAGs were collected, dried under high vacuum, and analyzed by NMR and matrix-assisted laser desorption-time of flight (MALDI-TOF) mass spectrometry. ^{1}H-NMR and ^{13}C-NMR spectra were acquired on Varian 300 MHz or 400 MHz spectrometers. Chemical shifts (δ; ppm) were reported against tetramethylsilane (0 ppm). MALDI-TOF mass spectroscopy was performed on a Voyager-DE PRO biospectrometry workstation (Applied Biosystems, Foster City, CA) using 2,5-dihydroxy benzoic acid as the matrix.

Ether-neutral lipid identification by ESI-MS

Adiposome lipid extracts (2.5 ml) were chromatographed on a 0.3 g silicic acid column packed in chloroform. The column was eluted with 10 ml of chloroform-methanol (98:2, v/v) to produce a neutral lipid fraction. The solvent was evaporated and the sample dissolved in 0.9 ml of chloroform. A 0.1 ml aliquot was diluted into 1.2 ml of chloroform-methanol-300 mM ammonium acetate in water (300:665:35) and introduced in the electrospray source of an Applied Biosystems API 4000 mass spectrometer as described below in Phospholipid Analysis. Q+ spectra were interpreted as TAGs. Product ion spectra of major TAG and MADAG species were determined using a collision energy of 45 V.

Phospholipid analysis

An automated electrospray ionization-tandem mass spectrometry approach was used, and data acquisition, analysis, and acyl group identification were carried out as described previously (13, 14) with minor modifications. An aliquot of extract (∼0.4 mg of lipid) was taken for mass spectrometry analysis. The lipid extract was combined with solvents and internal standards, such that the ratio of chloroform-methanol-300 mM ammonium acetate in water was 300:665:35 and the final volume was 1 ml. Internal standards, obtained and quantified as described previously (14),

were 0.66 nmol of di14:0-PC, 0.66 nmol of di24:1-PC, 0.66 nmol
of 13:0-lysoPC, 0.66 nmol of 19:0-lysoPC, 0.36 nmol of di14:0-PE,
0.36 nmol of di24:1-PE, 0.36 nmol of 14:0-lysoPE, 0.36 nmol of
18:0-lysoPE, 0.36 nmol of di14:0-phosphatidic acid (PA), 0.36 nmol
of di20:0(phytanoyl)-PA, 0.24 nmol of di14:0-PS, 0.24 nmol of
di20:0(phytanoyl)-PS, 0.20 nmol of 16:0-18:0-PI, and 0.16 nmol
of di18:0-PI.

Unfractionated lipid extracts were introduced by continuous
infusion into the ESI source on a triple quadrupole MS/MS sys-
tem (API 4000; Applied Biosystems). Samples were introduced
using an autosampler (LC Mini PAL; CTC Analytics AG, Zwingen,
Switzerland) fitted with the required injection loop for the ac-
quisition time and presented to the ESI needle at 30 μl/min.
The collision gas pressure was set at 2 (arbitrary units). The
collision energies, with nitrogen in the collision cell, were 28 V
for PE, 40 V for PC and SM, -58 V for PI, -57 V for PA, and
-34 V for PS. Declustering potentials were 100 V for PE, SM,
and PC and -100 V for PA and PI. Entrance potentials were
15 V for PE, 14 V for PC and SM, and -10 V for PI, PA, and
PS. Exit potentials were 11 V for PE, 14 V for PC, -15 V for PI,
-14 V for PA, and -13 V for PS. The mass analyzers were ad-
justed to a resolution of 0.7 amu full width at half height. For
each spectrum, 9–150 continuum scans were averaged in mul-
tiple channel analyzer mode. The source temperature (heated
nebulizer) was 100°C, the interface heater was on, $+5.5$ kV or
-4.5 kV was applied to the electrospray capillary, the curtain gas
was set at 20 (arbitrary units), and the two ion source gases were
set at 45 (arbitrary units).

Lipid species were detected using the scans described pre-
viously, including neutral loss of 87 in the negative mode for
PS (14, 15). Sequential precursor and neutral loss scans of the
extracts produce a series of spectra with each spectrum revealing
a set of lipid species containing a common head group fragment.
SM was determined from the same mass spectrum as PC (pre-
cursors of m/z 184 in positive mode) (15, 16) and by comparison
with PC internal standards using a molar response factor for
SM (in comparison with PC) determined experimentally to be
0.37. The background of each spectrum was subtracted, the data
were smoothed, and the peak areas were integrated using a
custom script and Applied Biosystems Analyst software. Isotopic
overlap corrections were applied, and the lipids in each class
were quantified in comparison with the two internal standards
of that class using corrected curves determined for the API 4000
mass spectrometer.

Other methods

Lipid droplets were purified from tissue culture cells by the
method of Liu et al. (3). To purify droplets from liver, a whole
mouse liver was sliced into small pieces in 20 ml of ice-cold
buffer containing 20 mM Tricine, pH 7.8, 250 mM sucrose,
and 100 μM PMSF. The sample was homogenized with a glass
Dounce homogenizer (20 strokes) on ice and centrifuged at
1,000 g for 10 min at 4°C. The supernatant fraction was trans-
ferred to two SW41 tubes, 7 ml each, and overlaid with 4 ml of
HEPES buffer (20 mM HEPES, pH 7.4, 100 mM KCl, and 2 mM
MgCl$_2$) and centrifuged at 40,000 rpm for 1 h at 4°C. After cen-
trifugation, the white band at the top of the tube was carefully
collected and further processed as described (3). To purify total
cell membranes, CHO K2 cells were cultured on 150 mm plates
to confluence, collected by scraping in ice-cold PBS with 100 μM
PMSF, and homogenized with a nitrogen bomb at 450 p.s.i. for
15 min on ice. The sample was centrifuged at 1,000 g for 10 min
at 4°C. The supernatant fraction was recovered and centrifuged
at 40,000 rpm in a SW41 tube for 1 h at 4°C to pellet all of
the membranes. The lipid composition of the pellet was de-
termined as described. Quantification of lipids on TLC plates

was by densitometric scanning of acidified, charred plates using
NIH ImageJ software, compared with quantitative TLC standards
(Nu-Chek Prep).

RESULTS

Initially, we set out to characterize the neutral lipid
composition of droplets purified from several different
cell types that had been grown in the presence or absence
of oleate. The baseline cell type for these studies was the
CHO K2 cell, which normally contains numerous droplets
(**Fig. 1A**, B, lane 2). Droplets were purified, and the lipids
were extracted and separated by TLC along with standards.
These droplets were rich in cholesteryl esters ($\sim$34%), TAG
($\sim$44%), and an unknown neutral lipid ($\sim$20%) that mi-
grated between cholesteryl esters and TAGs. Small amounts
of free fatty acids, cholesterol, and phospholipids also were
detected. The relative amounts of the major lipid classes
changed little when CHO K2 cells were grown overnight in
the presence of 80 μM oleate (Fig. 1A, B, lane 3). Moreover,
the same relative proportions of neutral lipids were found
in droplets isolated from NRK and SV589 cells that had
been grown in the presence of oleate (Fig. 1A, B, lanes 4, 5).

We used LC-APCI-MS/MS to identify the dominant
fatty acid species in the TAG fraction (see supplementary
Table I). The acyl composition was consistent with the
fatty acids typically found in mammalian cells, including
palmitic acid (P), stearic acid (S), oleic acid (O), linoleic
acid (L), and linolenic acid (Ln). Based on $[M+H]^+$ ions
and diagnostic fragment ions (representing the DAG por-
tion of the molecule), four major TAG species in CHO K2
cell lipid droplets were LLP, LLnO, LLO, and LLS. Mass
spectrometric (MALDI-TOF-MS) and NMR (^{1}H-NMR and
^{13}C-NMR) analyses showed that the cholesteryl ester frac-
tion contained at least three species: cholesteryl palmitate,
cholesteryl linoleate, and cholesteryl oleate (data not shown).

Droplets are rich in MADAG

The unusual neutral lipid migrating between cholesteryl
esters and TAG yielded $[M+H]^+$ ions by APCI-MS/MS
that were distinctly different from TAGs. An accurate mass
measurement by MALDI-TOF-MS of one major species
in this fraction was 865.7654, which suggested the for-
mula of a large hydrocarbon containing five oxygen atoms.
These data, along with key fragmentation ions identified
by APCI-MS, were consistent with the possibility that this
neutral lipid was a MADAG (see supplementary Table II).

To unequivocally identify the unknown neutral lipid,
we used NMR spectroscopy and additional mass spec-
trometry techniques. We purified the neutral lipid by silica
gel flash chromatography and determined the ^{1}H-NMR
spectrum. The spectrum showed peaks that were character-
istic of an esterified glycerol backbone (**Fig. 2A**, peaks b, c)
containing an ether linkage at a terminal carbon (Fig. 2A,
peaks a, d). This was supported by two-dimensional ^{1}H-^{1}H
correlation spectroscopy (Fig. 2B), in which all peaks could
be interpreted by proton signals of an ether lipid contain-
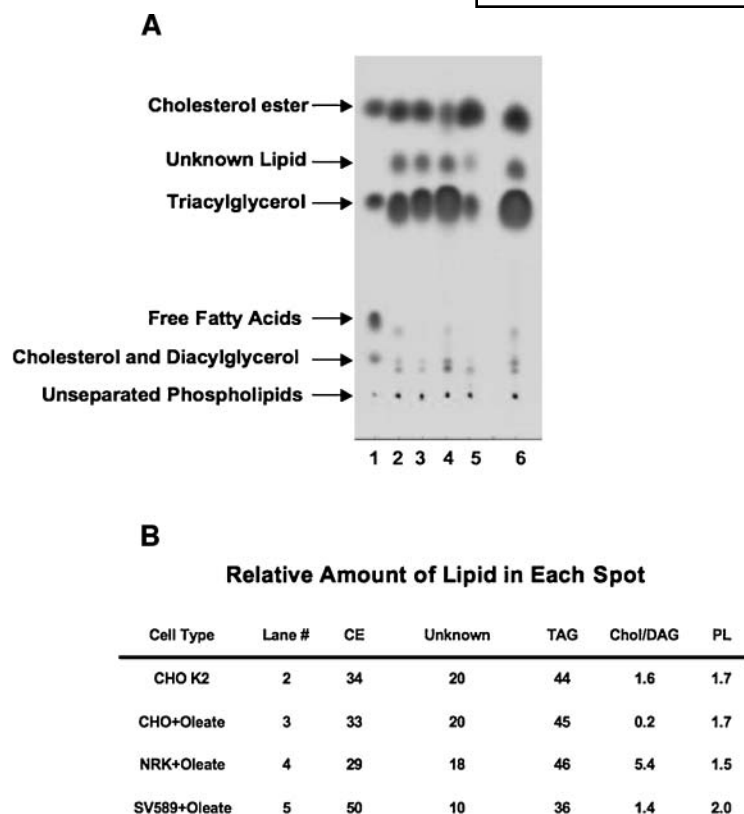ing unsaturated alkyl and acyl chains.

A

Fig. 1. Identification of lipid classes in droplets isolated from various cell types. A: Chromatographic separation of lipids from purified droplets. The indicated cell types (see B) were incubated for 16 h in the presence or absence of 100 μM oleate for NRK cells and 80 μM for the other cells. Droplets were isolated as described, and the indicated amount of lipid was separated on silica gel thin-layer chromatography using hexane-diethyl ether-acetic acid (80:20:1) as a solvent. Lane 1, standards. From top to bottom: cholesteryl oleate, triacylglycerol (TAG), oleic acid, cholesterol, and phosphatidylcholine (PC). Lane 2, droplets from untreated CHO cells (∼150 μg/lane). Lane 3, droplets from CHO cells grown overnight in the presence of oleate (∼150 μg/lane). Lane 4, droplets from NRK cells grown overnight in the presence of oleate (∼150 μg/lane). Lane 5, droplets from SV589 cells grown overnight in the presence of oleate (∼150 μg/lane). Lane 6, droplets from CHO cells (∼320 μg/lane). A trace of FFAs was detected in several preparations. Polar lipids including phospholipids remained at the origin in this solvent system. Lipids were visualized with iodine vapors. B: Relative amount (%) of the major lipid classes. Quantification was by densitometric scanning of acidified, charred plates using NIH ImageJ software, compared with quantitative TLC standards (Nu-Chek Prep). Unknown neutral lipid was quantified against a TAG standard curve. CE, cholesteryl ester; Chol/DAG, cholesterol/diacylglycerol; PL, phospholipid.

B

Relative Amount of Lipid in Each Spot

Cell Type	Lane #	CE	Unknown	TAG	Chol/DAG	PL
CHO K2	2	34	20	44	1.6	1.7
CHO+Oleate	3	33	20	45	0.2	1.7
NRK+Oleate	4	29	18	46	5.4	1.5
SV589+Oleate	5	50	10	36	1.4	2.0

ESI-MS/MS analysis of the neutral lipids from adiposomes revealed >100 species of TAGs and MADAGs (**Fig. 3A**). The $[M+NH_4]^+$ molecular ions represent an identifiable series of TAGs with intervening series of MADAGs in the same total ion chromatogram. Each species differs in mass by one oxygen atom, which represents mixed acyl species consistent with TAG and MADAG species predicted from LC-MS and MALDI-TOF-MS preliminary analyses (see supplementary Tables I, II). A list of TAG and MADAG species with increasing numbers of acyl/alkyl carbons and carbon-carbon double bonds is provided in supplementary Table III.

Product ion spectra of TAG and MADAG molecular ions confirmed the nature of the alk(en)yl or acyl groups in the parent ions (Fig. 3B, C). For example, the diacyl moieties derived from the neutral loss of one ammoniated fatty acid revealed the nature of the TAG at nominal mass m/z 900 as a mixture of several species with combinations of different acyl chains totaling 54:4 (Fig. 3B). The acyl groups were consistent with the principal TAGs at this mass being a mixture of 18:1/18:1/18:2, 18:0/18:2/18:2, and 16:0/20:2/18:2 (as well as several less abundant combinations). Similar patterns were seen with product ion scans of the ether neutral lipid species, and Fig. 3C shows a product ion scan derived from the ammoniated e52:3 parent ion. Here, the diacyl or alk(en)yl/acyl products with a neutral loss of ammoniated fatty acid or ammoniated fatty alcohol helped to identify the mixture of species that make up the principal e52:3 MADAG species. There were several possible combinations, but two major species

of e52:3 that are consistent with the fragment spectra are e18:1/16:0/18:2 and e16:0/18:1/18:2. The $[M+NH_4]^+$ TAGs and MADAGs identified in ESI-MS analyses were consistent with several species tentatively identified by LC-APCI-MS (see supplementary Tables I, II). The TAG shown in Fig. 3B corresponds to the $[M+H]^+$ ion with nominal m/z 883 in supplementary Table I, and the MADAG shown in Fig. 3C corresponds to the $[M+Na]^+$ ion with nominal m/z 865 in supplementary Table II.

Finally, we compared the ^{13}C-NMR spectrum of the purified neutral lipid species with the spectrum of pure glycerol trioleate. Two major differences were noted between the two spectra (see supplementary Fig. I). The ^{13}C-NMR spectrum of the purified lipid had two additional peaks between 62 and 73 ppm (see supplementary Fig. IA, B; compare top and bottom spectra), consistent with the presence of an ether linkage in a terminal carbon glycerol backbone. Only one peak was seen in this region of glycerol trioleate (see supplementary Fig. IA, B, top spectra). The purified lipid also contained seven or more peaks between 127 and 131 ppm (see supplementary Fig. IC, bottom spectra). ^{13}C peaks in this region correspond to unsaturated carbon atoms in a double bond. Glyceryl trioleate has only two peaks in this region because all acyl chains in this molecule are oleate, and oleate contains only one double bond (see supplementary Fig. IC, top spectra). The presence of multiple peaks indicated that the fraction contains different alkyl/acyl chains of mixed unsaturation. We conclude that the unknown neutral lipid is a mixture of MADAG (ether neutral lipid)
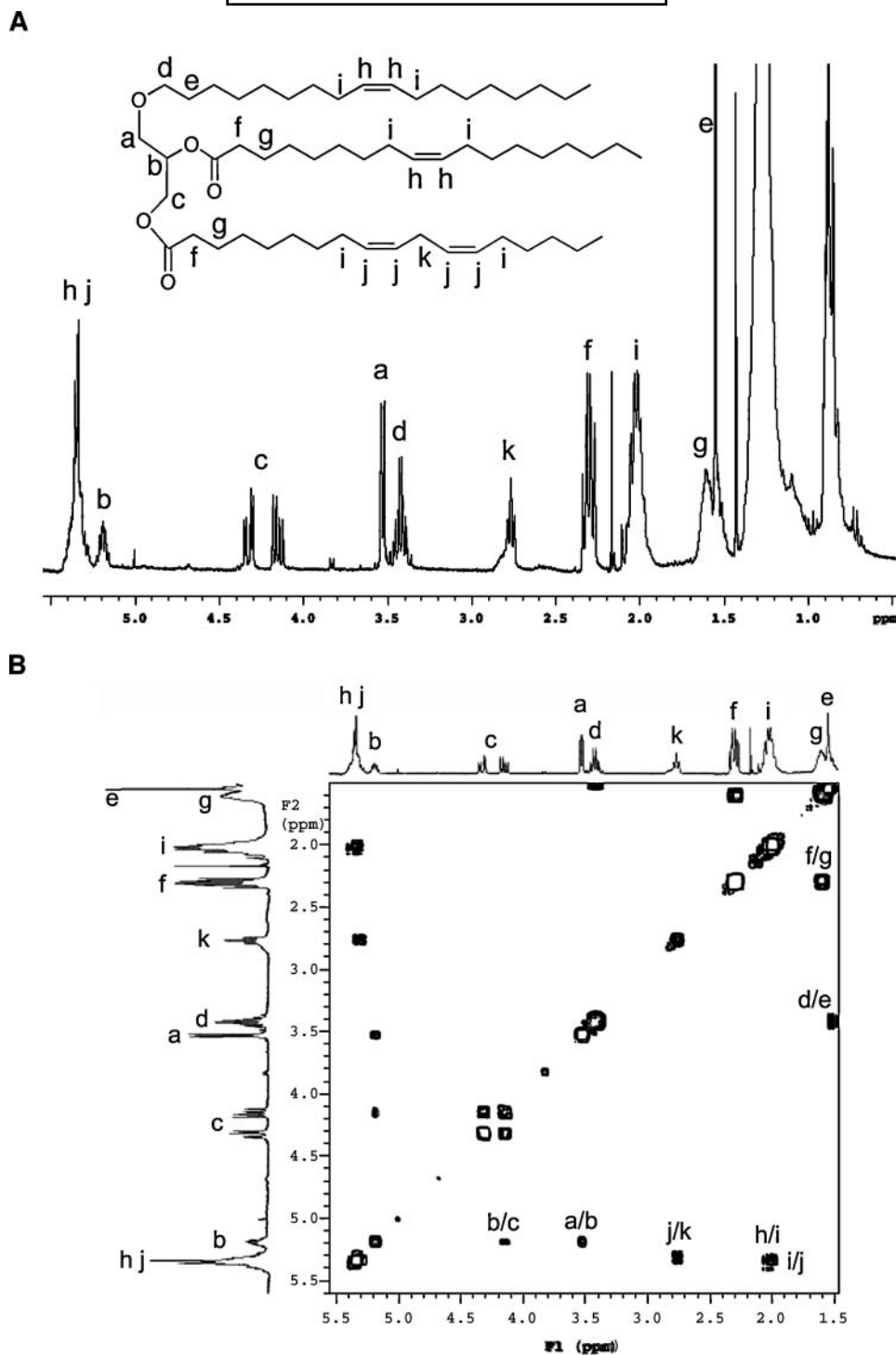
Fig. 2. NMR analysis of unknown neutral lipids. A: ^{1}H-NMR spectrum of the purified unknown neutral lipid species. The spectral data are consistent with a mixture of ether-linked neutral lipid species. The inset shows the structure of a monoalk(en)yl diacylglycerol (MADAG) species of the formula weight (868.79) consistent with a mass peak found by matrix-assisted laser desorption-time of flight mass spectroscopy (see supplementary Table II). Protons with chemical shifts of >1.5 ppm are assigned. The same letters are used to indicate protons with the same or nearly the same chemical shifts. Both the chain length and the degree of unsaturation are assigned arbitrarily to the fatty acyl and alkyl chains. We did not observe any peaks between 6.0 and 6.5 ppm, so we were unable to detect the presence of vinyl ether lipid. B: Two-dimensional [1]H-^{1}H correlation spectroscopy spectrum of the purified neutral lipid class. Cross peaks are labeled to indicate pairs of spin-coupled protons of >1.5 ppm. Spectral data support the structural identification from one-dimensional ^{1}H-NMR in A.
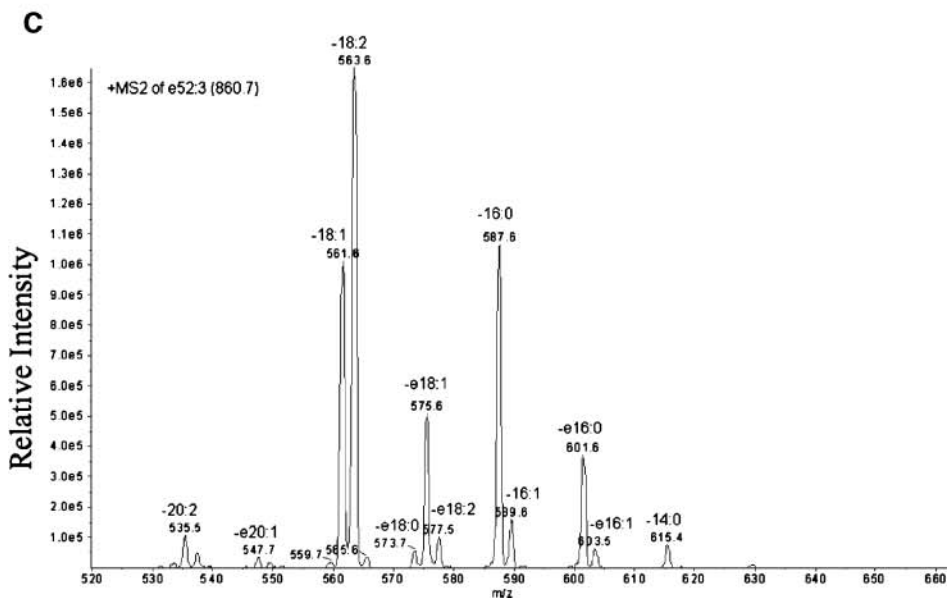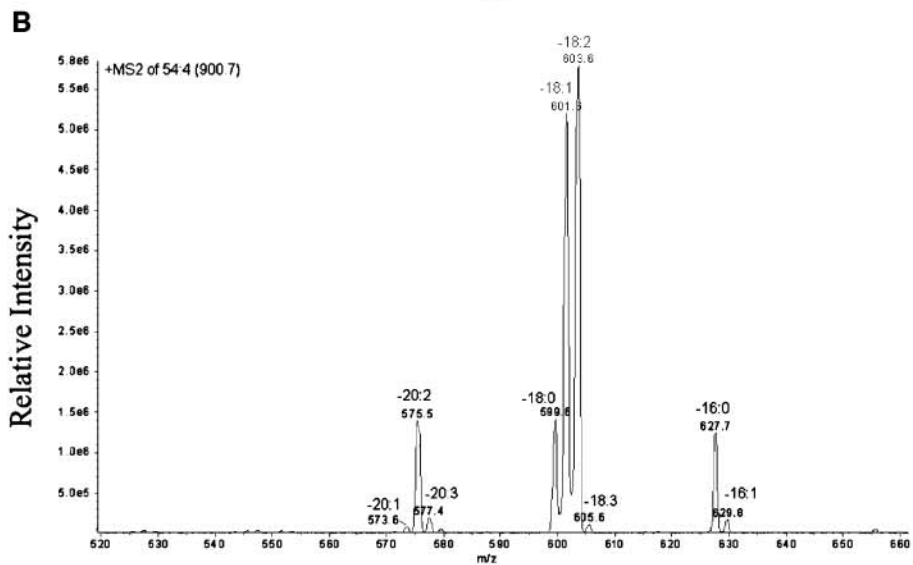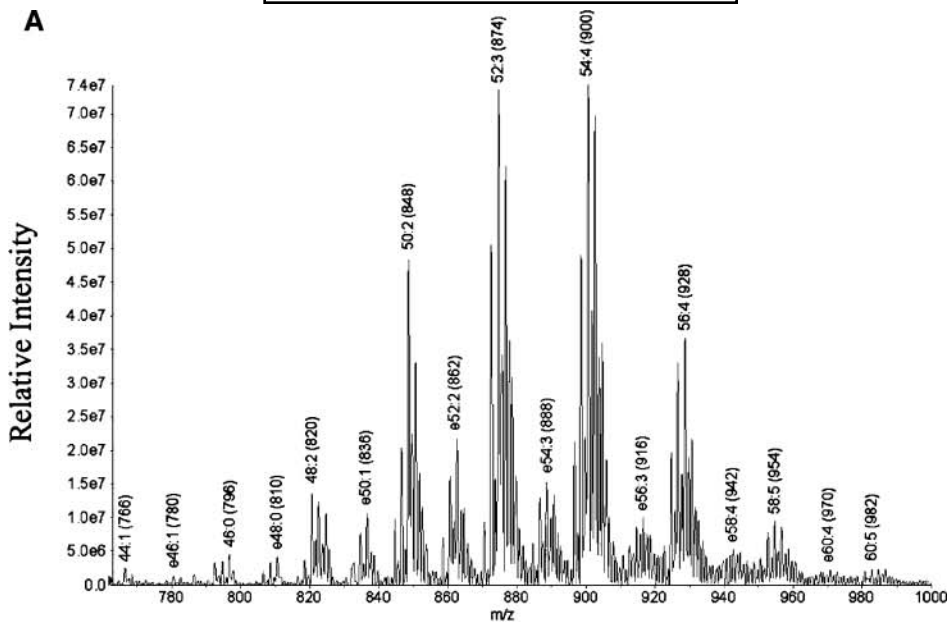
molecular species containing alkyl and acyl chains of various lengths and degrees of unsaturation. In addition to physiologically relevant unsaturated fatty acids, such as 16:1, 18:1, 18:2, 18:3, and 20:4, the mixture may also contain saturated fatty acids, including 14:0, 16:0, and 18:0. This conclusion is supported by ESI-MS analyses of precursor and product ion scans (Fig. 3 and supplementary Table III).

MADAG was not present in all cell types. The key step in the synthesis of ether lipids is the conversion of acyl-dihydroxyacetone phosphate (DHAP) to alkyl-DHAP by the peroxisomal enzyme alkyl-DHAP synthase (17). Therefore, droplets isolated from cells lacking peroxisomes should contain reduced amounts of MADAG. To determine whether this is correct, we used primary fibroblasts from patients with Zellweger syndrome, which lack functional peroxisomes owing to a defect in peroxisome assembly (18). CHO K2 cells (**Fig. 4A**, lane 1) as well as normal (lane 2) and Zellweger (lane 3) human fibroblasts grown for 48 h in the presence of 80 μM oleate were processed to extract lipids from isolated droplets. The MADAG band was present in droplets isolated from normal cells but markedly reduced in Zellweger cells. We also compared the relative amount of MADAG in lipids extracted from adipose tissue (Fig. 4B) and found that MADAG was not detected in either white (lane 2) or brown (lane 3) adipose tissue. Previous studies have shown that during adipocyte differentiation, the level of alkyl-DHAP synthase declines (19), which may explain the low amounts of MADAG in adipose neutral lipids. Indeed, very little MADAG was found in droplets isolated from differentiated 3T3-L1 cells (Fig. 4B, lane 5), whereas undifferentiated 3T3-L1 cells grown overnight in the presence of oleate had significant amounts of MADAG (Fig. 4B, lane 4). We also detected MADAG in droplets isolated from liver (Fig. 4B, lane 8, arrowhead). Liver droplets were also rich in lipid species that migrate with the relative mobility values of retinoic ester (Fig. 4B, lane 8, asterisk) and free fatty acid (Fig. 4B, lane 8, double asterisk). Finally, we noted that droplets from NRK cells (Fig. 4B, lane 6) as well as NIH 3T3 cells grown in oleate (Fig. 4B, lane 4) contained low amounts of cholesteryl ester but still had considerable amounts of MADAG, which indicates that droplets accumulate these esters independently. These results emphasize two points. First, ether lipid metabolism varies among cell types and, most likely, is dependent on a cooperative interaction between peroxisomes and adiposomes. Second, adiposomes accumulate different types of neutral lipids depending on the specialized function of the cell.

Droplets have a unique phospholipid profile

Although the proportion of total phospholipids in droplets is small relative to neutral lipids (1–2% of total), phospholipids stabilize the droplet and serve as an interface with other cellular compartments. Recent sensitive mass spectrometric techniques (ESI-MS/MS) have made it possible to identify and quantify phospholipid classes as well as the amount of specific molecular species in each class (20). We used direct infusion ESI followed by MS/MS to identify different classes of polar lipids in the droplet and quantify the amount of the molecular species within each class. The species in each head group class are detected as the head group fragment produced by collision-induced dissociation. Classes are detected by sequential scans during continuous infusion, and quantification is done using internal standards for each head group class (13, 14) (a typical spectrum for phosphocholine-containing phospholipids is shown in supplementary Fig. II). The phospholipids in the major classes were determined in two different droplet preparations (**Fig. 5A**). PC and PE were the most abundant phospholipids, followed by PI, ePC, and ePE. Lower levels of lysophospholipids (lysoPC and lysoPE), SM, PA, and PS also were detected.

Detailed profiles of the different lipid species within each major class are shown in supplementary Figs. III, IV. More than 85% of the total diacyl PC pool (out of a total of 50 molecular species) was composed of seven principal types: 34:2, 34:3, 36:4, 36:3, 36:2, 38:4, and 38:3 (total acyl carbons:total acyl double bonds; see supplementary Fig. IIIA), whereas the major ePCs were 34:2, 34:1, and 36:3 (see supplementary Fig. IIIB) and the dominant lysoPC was 18:2 (see supplementary Fig. IIIC). We detected 45 species of PE (see supplementary Fig. IVA), and this PE pool was dominated by 36:3 and 36:2, whereas we quantified 24 species of ePE (see supplementary Fig. IVB), and these were mostly 36:3, 36:2, and 38:5. There were 10 lysoPE species detected, and this class was dominated by

Fig. 3. Electrospray ionization-mass spectrometry (ESI-MS) of neutral lipids (TAG and MADAG). Neutral lipids were fractionated by silica gel chromatography and analyzed in chloroform-methanol-300 mM ammonium acetate in water (300:665:35, v/v/v). A: The peaks represent the $[M+NH_4]^+$ ions, corresponding to the TAGs and MADAGs. The largest peak in each cluster is identified according to total acyl/alk(en)yl carbons:total carbon-carbon double bonds, with the "e" (for ether) representing the presence of an alk(en)yl chain (in an ether linkage to the glycerol). The masses shown in parentheses are the nominal masses of the $[M+NH_4]^+$ ions. The arrows designate the two molecular species for which product ion scans are shown in B and C. B: The peaks represent the product ion spectrum derived from the TAG 54:4 (nominal mass of 900). Based on acyl ion losses, some likely molecular species of the TAG 54:4 include 18:1/18:2/18:1, 18:2/18:2/18:0, and 20:2/18:2/16:0. C: The peaks represent the product ion spectrum derived from the MADAG e52:3 (nominal mass of 860). Based on acyl/alkyl losses, the combinations of fatty acid/alcohol that might make up MADAG e52:3 include e18:1/18:2/16:0 and e16:0/18:2/18:1. The product ion spectra in B and C show the neutral loss of ammoniated fatty acids or ammoniated fatty alcohols (indicated with "e"). Each of the "e" MADAG species in A for which we examined product ion spectra showed the characteristic neutral loss of ammoniated alcohols as well as the neutral loss of ammoniated fatty acids, whereas the product ion scans of TAGs showed only neutral losses of ammoniated fatty acids.
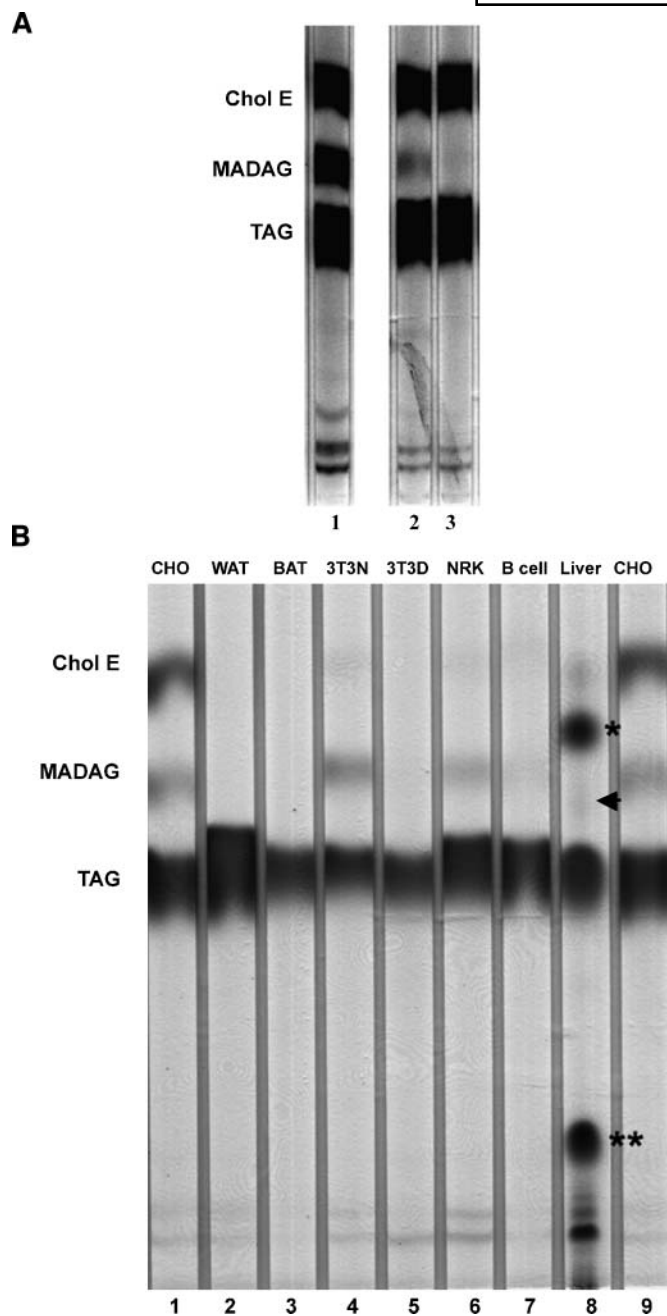
Fig. 4. Not all cells contain MADAG. A: CHO cells (lane 1) grown in medium alone and human fibroblasts (lane 2) and Zellweger primary human fibroblasts (lane 3) grown for 48 h in the presence of 80 μM oleate. Droplets isolated from Zellweger cells had nearly undetectable levels of MADAG. B: Neutral lipid profiles of droplets isolated from CHO cells (lanes 1, 9), undifferentiated 3T3-L1 cells grown in the presence of 80 μM oleate (3T3N; lane 4), differentiated 3T3-L1 cells (3T3D; lane 5), NRK cells (lane 6) and B-cells (lane 7) grown overnight in the presence of oleate, and liver (lane 8). Also shown are the neutral lipid profiles of lipids extracted from white adipose tissue (WAT; lane 2) and brown adipose tissue (BAT; lane 3). The migration points of retinoic acid (asterisk) and fatty acid (double asterisk) are indicated. The faint band between retinoic acid and TAG (arrowhead) corresponds to MADAG. Chol E, cholesteryl ester.
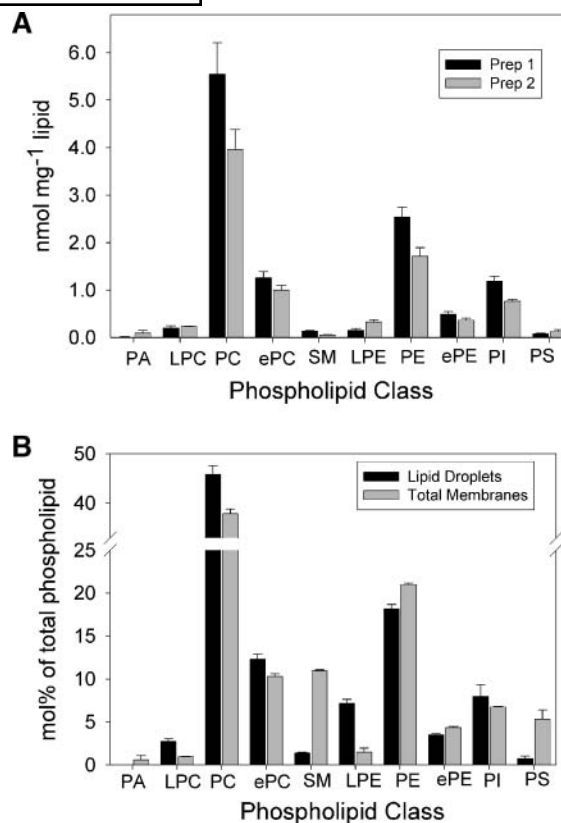

Fig. 5. Identification and quantification of phospholipids in droplets and their relative amounts compared with total membranes. A: Amounts were summed from individual molecular species amounts and represent averages and SDs of five replicate extractions from two independent organelle isolations [preparations (Prep) 1 and 2]. Amounts of lysophospholipids and phosphatidylinositol (PI) varied somewhat from preparation to preparation. B: Amounts were summed from individual molecular species amounts and represent averages of five replicate extractions plotted as mol% of total phospholipids, so that comparisons can be made between droplets and total membranes (postnuclear membranes). Droplets were proportionately higher in PC, lysoPC (LPC), and lysophosphatidylethanolamine [lysoPE (LPE)] but much lower in sphingomyelin (SM) and phosphatidylserine (PS). Values were obtained by ESI-MS/MS direct infusion experiments, and quantification was based on internal standards as described in Materials and Methods. PA, phosphatidic acid; ePC, ether-linked phosphatidylcholine; ePE, ether-linked phosphatidylethanolamine; PE, phosphatidylethanolamine.

18:2, 18:1, and 20:2 (see supplementary Fig. IVC). In comparison with PC and PE, the PI profile was relatively simple, with only nine species (mostly 38:4; see supplementary Fig. IVD). We conclude that the phospholipid composition of adiposomes is surprisingly complex, with ~160 molecular species in seven classes. Phospholipid classes, such as SM and PS, although detectable, were present at extremely low levels in droplets; therefore, we did not quantify species within these classes.

We also compared the concentration of phospholipid classes in droplets versus total membranes (Fig. 5B). The mol% phospholipid composition of the isolated droplet was generally similar to that of cell membranes, with the

exception that droplets had significantly more PC, lysoPC, and lysoPE and very low levels of SM and PS. Because lyso-phospholipids were considerably more enriched than PC, we compared the mol% of lysoPC and lysoPE species in droplets with total membrane phospholipids (**Fig. 6A, B**). Droplets were higher in lysoPC species 16:0, 18:2, 18:1, and 20:2. Likewise, lysoPE in droplets was higher in the same fatty acid chains and, in addition, 20:4 and 20:1. On the other hand, when we compared each species in the droplet with the total amount of that species among all membrane phospholipid (Fig. 6C, D), only lysoPC 18:2 was enriched in droplets. Thus, although droplets contain more lysoPC and lysoPE relative to all membrane phospholipids, among all lysophospholipids in the cell they are selectively enriched in lysoPC 18:2 and reduced in lysoPC 16:0 and 18:0. Collectively, these results indicate that there are distinctive class and molecular species differences between the phospholipid monolayer covering the droplet surface and the total membrane phospholipid bilayer in the cell. These differences suggest that the phospholipids surrounding each droplet are specialized to carry out specific metabolic and lipid-trafficking functions of the adiposome.

DISCUSSION

Mass spectrometry has dramatically increased our ability to obtain detailed information about the lipid composition of cellular and subcellular compartments. ESI-MS has proven to be particularly well suited for lipid analysis because direct infusion of a biological extract combined with internal standards allows for the quantification of polar lipid species from the mass spectra (21). To quantify the lipids by mass spectrometry (20), we used two internal standards for each lipid class to identify the species of the class from the precursor or neutral loss scans, based on a head group fragment. Although this approach is straightforward, it should be noted that some lipid species, particularly those containing ether bonds, might have a propensity to form a
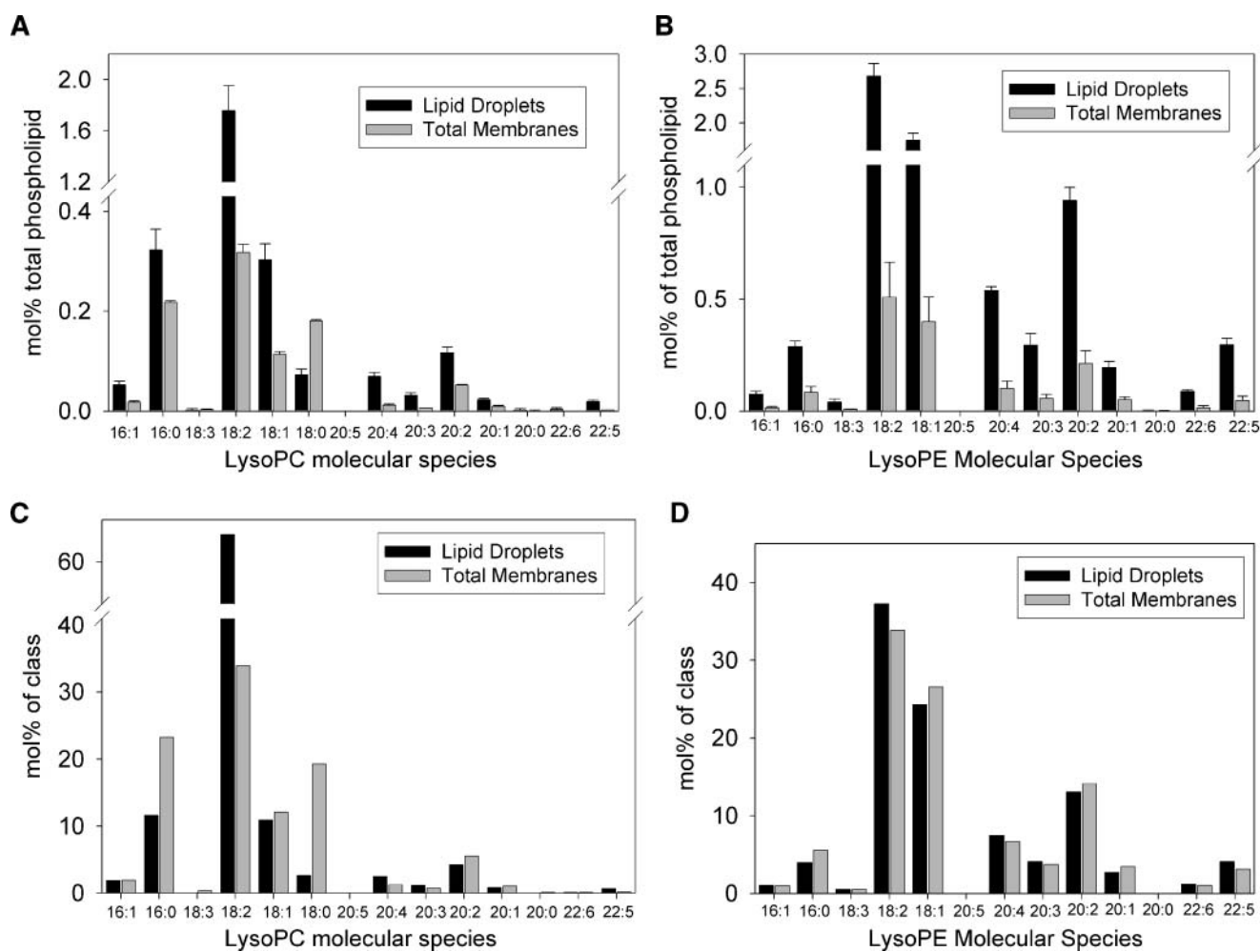

Fig. 6. Comparative amounts of lysoPC and lysoPE in droplets and total membranes. Amounts were calculated as mol% of total phospholipids (A, B), mol% of the lysoPC class (C), or mol% of the lysoPE class (D). A, B: Average and SD of five replicate extractions. C, D: Percentage of individual species as a molar fraction of the lysoPC or lysoPE class, respectively. LysoPC 18:2 was enriched 2-fold in droplets relative to membranes, whereas 16:0 and 18:0 appeared to be preferentially excluded (50% and 90% reductions, respectively). Values were obtained by ESI-MS/MS direct infusion experiments and quantification using internal standards as described.

different head group fragment than the diacyl internal standard. This potential issue with quantification needs to be resolved once better standard compounds become available. Recently, mass spectrometry has been used to analyze phospholipids secreted by type II alveolar epithelial cells in culture (22), the effects of knocking down 1-acylglycerol-3-phosphate-O-acyltransferase 2 with small interfering RNA on the phospholipid and TAG composition of differentiating adipocytes (23), and phospholipids in lipid rafts containing epidermal growth factor receptor (24).

ESI-MS/MS analysis has revealed that the phospholipid composition of isolated droplets is remarkably complex. PC was the dominant phospholipid class, in agreement with previous studies (25). We detected >50 different species of PC. Likewise, we detected 45 species of PE and 9 species of PI. We also detected a variety of lyso- and ether-linked derivatives of PC and PE. On the other hand, very little PS or SM was found in the purified droplet. The concentration of certain species of lysophospholipids was higher in the droplets than in total cell membranes. For example, lysoPC 16:0, 18:2, and 18:1 were enriched in the droplets relative to total membrane phospholipid, but lysoPC 18:0 was deficient. HepG2 cells appear to be enriched in lysoPC 18:1 (25), which indicates that all droplets may be enriched in lysoPC but the major fatty acid varies with cell type and growth conditions. The rich assortment of phospholipids suggests that the phospholipid monolayer that surrounds each droplet is more than a simple container for neutral lipids. The diversity of phospholipids suggests that adiposomes may have an important function in supplying both phospholipids for membrane lipid turnover and signaling lipids that control critical metabolic pathways (26).

In addition to detecting >160 phospholipid species in isolated droplets, we also found a significant amount of MADAG in many droplet preparations. MADAG was prevalent in droplets isolated from both tissue culture cells and liver but not in lipids extracted from adipose tissue or in droplets isolated from differentiated NIH 3T3-L1 cells. The prevalence of MADAGs suggests a role for adiposomes in ether lipid metabolism. The first three enzymes in ether lipid biosynthesis are in peroxisomes (17, 19, 27). The conversion of 1-alkylglycerol-3-phosphate to 1-alkyl-2-acyl-glycerol, however, is thought to occur in the endoplasmic reticulum (18). Most likely, it is the 1-alkyl-2-acyl-glycerol that is converted to MADAG (possibly by a 1,2-diacylglycerol acyltransferase) for storage in the droplet. We speculate that MADAG can be converted to phospholipid because several major MADAG molecular species identified by NMR and MS (Figs. 2, 3; see supplementary Fig. I and supplementary Tables II, III) had similar alkyl/acyl composition to the ether phospholipids present in the droplet. For example, we identified MADAGs with the structure e18:1/18:2/16:0 (Fig. 3C; see supplementary Tables II, III), which could be the precursor to or derived from 36:3 ePC or ePE (with e18:1/18:2 at the sn-1/2 positions). We cannot determine whether these phospholipids have an alkyl or an alkenyl linkage at the sn-1 position. Nevertheless, the adiposome may function both as a supply depot for ether

phospholipid biosynthesis and as a recovery organelle for storage, much like the interconversion of phospholipids and TAGs (28, 29). Indeed, the greater amount of lysophospholipids in droplets also indicates a role for adiposomes in phospholipid recycling. The dependence on peroxisomes for ether lipid biosynthesis also suggests a metabolic interaction between the two organelles, consistent with recent studies demonstrating that in yeast the peroxisomes and droplets interact physically (30).

In conclusion, the lipid profile of the isolated droplet reveals a surprising complexity in phospholipid species as well as a novel role for the organelle in the compartmentalization of an underappreciated ether neutral lipid. These results suggest that adiposomes have a function in coordinating the metabolism and trafficking of lipids between subcellular compartments. We have found that lipidomics offers a valuable insight into the behavior of different classes and species of droplet lipids. This method promises to be an essential tool for dissecting the function of the adiposome in lipid droplet ontogeny and intracellular lipid metabolism.

REFERENCES

1. van Meer, G. 2001. Caveolin, cholesterol, and lipid droplets? *J. Cell Biol.* **152:** F29–F34.
2. Beckman, M. 2006. Cell biology. Great balls of fat. *Science.* **311:** 1232–1234.
3. Liu, P., Y. Ying, Y. Zhao, D. I. Mundy, M. Zhu, and R. G. Anderson. 2004. Chinese hamster ovary K2 cell lipid droplets appear to be metabolic organelles involved in membrane traffic. *J. Biol. Chem.* **279:** 3787–3792.
4. Athenstaedt, K., D. Zweytick, A. Jandrositz, S. D. Kohlwein, and G. Daum. 1999. Identification and characterization of major lipid particle proteins of the yeast *Saccharomyces cerevisiae. J. Bacteriol.* **181:** 6441–6448.
5. Katavic, V., G. K. Agrawal, M. Hajduch, S. L. Harris, and J. J. Thelen. 2006. Protein and lipid composition analysis of oil bodies from two *Brassica napus* cultivars. *Proteomics.* **6:** 4586–4598.

6. Brasaemle, D. L., G. Dolios, L. Shapiro, and R. Wang. 2004. Proteomic analysis of proteins associated with lipid droplets of basal and lipolytically stimulated 3T3-L1 adipocytes. *J. Biol. Chem.* **279:** 46835–46842.

7. Fujimoto, Y., H. Itabe, J. Sakai, M. Makita, J. Noda, M. Mori, Y. Higashi, S. Kojima, and T. Takano. 2004. Identification of major proteins in the lipid droplet-enriched fraction isolated from the human hepatocyte cell line HuH7. *Biochim. Biophys. Acta.* **1644:** 47–59.

8. Murphy, D. J. 2001. The biogenesis and functions of lipid bodies in animals, plants and microorganisms. *Prog. Lipid Res.* **40:** 325–438.

9. Michaely, P., W. P. Li, R. G. Anderson, J. C. Cohen, and H. H. Hobbs. 2004. The modular adaptor protein ARH is required for low density lipoprotein (LDL) binding and internalization but not for LDL receptor clustering in coated pits. *J. Biol. Chem.* **279:** 34023–34031.

10. Bligh, E. G., and W. J. Dyer. 1959. A rapid method of total lipid extraction and purification. *Can. J. Biochem. Physiol.* **37:** 911–917.

11. Chapman, K. D., and T. S. Moore, Jr. 1993. N-Acylphosphatidylethanolamine synthesis in plants: occurrence, molecular composition, and phospholipid origin. *Arch. Biochem. Biophys.* **301:** 21–33.

12. Folch, J., M. Lees, and G. H. Sloane Stanley. 1957. A simple method for the isolation and purification of total lipides from animal tissues. *J. Biol. Chem.* **226:** 497–509.

13. Wanjie, S. W., R. Welti, R. A. Moreau, and K. D. Chapman. 2005. Identification and quantification of glycerolipids in cotton fibers: reconciliation with metabolic pathway predictions from DNA databases. *Lipids.* **40:** 773–785.

14. Welti, R., X. Wang, and T. D. Williams. 2003. Electrospray ionization tandem mass spectrometry scan modes for plant chloroplast lipids. *Anal. Biochem.* **314:** 149–152.

15. Brugger, B., G. Erben, R. Sandhoff, F. T. Wieland, and W. D. Lehmann. 1997. Quantitative analysis of biological membrane lipids at the low picomole level by nano-electrospray ionization tandem mass spectrometry. *Proc. Natl. Acad. Sci. USA.* **94:** 2339–2344.

16. Liebisch, G., B. Lieser, J. Rathenberg, W. Drobnik, and G. Schmitz. 2004. High-throughput quantification of phosphatidylcholine and sphingomyelin by electrospray ionization tandem mass spectrometry coupled with isotope correction algorithm. *Biochim. Biophys. Acta.* **1686:** 108–117.

17. van den Bosch, H., and E. C. de Vet. 1997. Alkyl-dihydroxyacetone-phosphate synthase. *Biochim. Biophys. Acta.* **1348:** 35–44.

18. Wanders, R. J. 2004. Peroxisomes, lipid metabolism, and peroxisomal disorders. *Mol. Genet. Metab.* **83:** 16–27.

19. Hajra, A. K., L. K. Larkins, A. K. Das, N. Hemati, R. L. Erickson, and O. A. MacDougald. 2000. Induction of the peroxisomal glycero-lipid-synthesizing enzymes during differentiation of 3T3-L1 adipocytes. Role in triacylglycerol synthesis. *J. Biol. Chem.* **275:** 9441–9446.

20. Welti, R., and X. Wang. 2004. Lipid species profiling: a high-throughput approach to identify lipid compositional changes and determine the function of genes involved in lipid metabolism and signaling. *Curr. Opin. Plant Biol.* **7:** 337–344.

21. Han, X., and R. W. Gross. 2005. Shotgun lipidomics: multidimensional MS analysis of cellular lipidomes. *Expert Rev. Proteomics.* **2:** 253–264.

22. Postle, A. D., L. W. Gonzales, W. Bernhard, G. T. Clark, M. H. Godinez, R. I. Godinez, and P. L. Ballard. 2006. Lipidomics of cellular and secreted phospholipids from differentiated human fetal type II alveolar epithelial cells. *J. Lipid Res.* **47:** 1322–1331.

23. Gale, S. E., A. Frolov, X. Han, P. E. Bickel, L. Cao, A. Bowcock, J. E. Schaffer, and D. S. Ory. 2006. A regulatory role for 1-acylglycerol-3-phosphate-O-acyltransferase 2 in adipocyte differentiation. *J. Biol. Chem.* **281:** 11082–11089.

24. Pike, L. J., X. Han, and R. W. Gross. 2005. Epidermal growth factor receptors are localized to lipid rafts that contain a balance of inner and outer leaflet lipids: a shotgun lipidomics study. *J. Biol. Chem.* **280:** 26796–26804.

25. Tauchi-Sato, K., S. Ozeki, T. Houjou, R. Taguchi, and T. Fujimoto. 2002. The surface of lipid droplets is a phospholipid monolayer with a unique fatty acid composition. *J. Biol. Chem.* **277:** 44507–44512.

26. D'Avila, H., R. C. Melo, G. G. Parreira, E. Werneck-Barroso, H. C. Castro-Faria-Neto, and P. T. Bozza. 2006. *Mycobacterium bovis* bacillus Calmette-Guerin induces TLR2-mediated formation of lipid bodies: intracellular domains for eicosanoid synthesis in vivo. *J. Immunol.* **176:** 3087–3097.

27. de Vet, E. C., L. Ijlst, W. Oostheim, C. Dekker, H. W. Moser, H. van Den Bosch, and R. J. Wanders. 1999. Ether lipid biosynthesis: alkyl-dihydroxyacetonephosphate synthase protein deficiency leads to reduced dihydroxyacetonephosphate acyltransferase activities. *J. Lipid Res.* **40:** 1998–2003.

28. Coleman, R. A., and D. P. Lee. 2004. Enzymes of triacylglycerol synthesis and their regulation. *Prog. Lipid Res.* **43:** 134–176.

29. Williams, M. L., R. A. Coleman, D. Placezk, and C. Grunfeld. 1991. Neutral lipid storage disease: a possible functional defect in phospholipid-linked triacylglycerol metabolism. *Biochim. Biophys. Acta.* **1096:** 162–169.

30. Binns, D., T. Januszewski, Y. Chen, J. Hill, V. S. Markin, Y. Zhao, C. Gilpin, K. D. Chapman, R. G. Anderson, and J. M. Goodman. 2006. An intimate collaboration between peroxisomes and lipid bodies. *J. Cell Biol.* **173:** 719–731.